Title: The properties of (Pb0.97Ba0.03)[(Zr0.98Ti0.02)1-zSnz]O3 ceramics with 0 < z < 0.08

Author: Dagmara Brzezińska, Ryszard Skulski, Paweł Wawrzała, Grzegorz Dercz

Citation style: Brzezińska Dagmara, Skulski Ryszard, Wawrzała Paweł, Dercz Grzegorz. (2013). The properties of (Pb0.97Ba0.03)[(Zr0.98Ti0.02)1-zSnz]O3 ceramics with 0 < z < 0.08. "Archives of Metallurgy and Materials" (Vol. 58, no. 4, (2013), s. 1377-1380), doi 10.2478/amm-2013-0178

A R C H I V E S O F M E T A L L U R G Y A N D M A T E R I A L S
Volume 58 2013 Issue 4
DOI: 10.2478/amm-2013-0178

D. BRZEZIŃSKA*, R. SKULSKI*, P. WAWRZAŁA*, G. DERCZ**

THE PROPERTIES OF $(Pb_{0.97}Ba_{0.03})[(Zr_{0.98}Ti_{0.02})_{1-z}Sn_z]O_3$ CERAMICS WITH $0 < z < 0.08$

WŁAŚCIWOŚCI CERAMIKI $(Pb_{0,97}Ba_{0,03})[(Zr_{0,98}Ti_{0,02})_{1-z}Sn_z]O_3$ O WARTOŚCIACH $0 < z < 0,08$

We present the results of obtaining and investigations of $(Pb_{1-x}Ba_x)((Zr_{1-y}Ti_y)_{1-z}Sn_z)O_3$ (PBZTS) ceramics with x =const =0.03, y =const=0.02, z =0, 0.02, 0.04, 0.06 and 0.08. Investigated compositions are close to rhombohedral-orthorhombic morphotropic phase boundary. Ceramic samples have been obtained by conventional ceramic technology from oxides PbO, ZrO_2, TiO_2, SnO_2 and barium carbonate $BaCO_3$. The calcined powders were crushed and next pressed into discs and sintered free sintering (FS) method. For such obtained samples the following investigations have been done: EDS, XRD, microstructure of fractured samples, dielectric measurements, *P-E*hysteresis loops investigations at various temperatures.

Keywords: PBZT and PBZTS ceramics, phase transitions, dielectric properties

Przedstawiono wyniki badań ceramiki $(Pb_{1-x}Ba_x)((Zr_{1-y}Ti_y)_{1-z}Sn_z)O_3$ (PBZTS) dla stałych wartości parametrów x =0,03 i y =0,02 oraz z =0, 0,02, 0,04, 0,06 i 0,08. Badane składy PBZTS znajdują się w pobliżu granicy fazowej między fazami o romboedrycznej i ortorombowej deformacji komórek elementarnych. Ceramiczne próbki PBZTS zostały otrzymane z prostych tlenków PbO, ZrO_2, TiO_2, SnO_2 i węglanu baru $BaCO_3$. Proszki po kalcynacji zostały rozdrobnione, a następnie uformowano z nich wypraski i zagęszczono metodą swobodnego spiekania (FS). Dla otrzymanych próbek PBZT/PBZTS przeprowadzono badania EDS, XRD, badania mikrostruktury przełamów, badania podstawowych właściwości dielektrycznych, badania pętli histerezy w różnych temperaturach.

1. Introduction

Lead containing perovskite-type oxides are very important for practical applications. Very good electromechanical properties of such materials are connected with the big amplitude of vibrations of the heaviest Pb-ion. [1, 2]. The properties of such ceramics depend on conditions of obtaining. (i.e. the methods of synthesis, purity of starting components, the degree of granulation, densification etc.) [3, 4]. First systematic investigations of $(Pb_{1-x}Ba_x)(Zr_{1-y}Ti_y)O_3$ solid solution (PBZT) were described in [5]. The phase diagram and another properties of PBZT were presented in works [5-8]. Below we describe a solid solution of $(Pb_{0.97}Ba_{0.03})(Zr_{0.98}Ti_{0.02})O_3$ with $PbSnO_3$ (Tab. 1). This composition is close to the boundary between orthorhombic and rhombohedral phases.

TABLE 1

The chemical compositions of investigated $(Pb_{0.97}Ba_{0.03})[(Zr_{0.98}Ti_{0.02})_{1-z}Sn_z]O_3$ ceramics (the assumed values)

Chemical compositions:
$(Pb_{0.97}Ba_{0.03})(Zr_{0.98}Ti_{0.02})O_3$
$(Pb_{0.97}Ba_{0.03})[(Zr_{0.98}Ti_{0.02})_{0.98}Sn_{0.02}]O_3 = (Pb_{0.97}Ba_{0.03})(Zr_{0.96}Ti_{0.02}Sn_{0.02})O_3$
$(Pb_{0.97}Ba_{0.03})[(Zr_{0.98}Ti_{0.02})_{0.96}Sn_{0.04}]O_3 = (Pb_{0.97}Ba_{0.03})(Zr_{0.94}Ti_{0.02}Sn_{0.04})O_3$
$(Pb_{0.97}Ba_{0.03})[(Zr_{0.98}Ti_{0.02})_{0.94}Sn_{0.06}]O_3 = (Pb_{0.97}Ba_{0.03})(Zr_{0.921}Ti_{0.019}Sn_{0.06})O_3$
$(Pb_{0.97}Ba_{0.03})[(Zr_{0.98}Ti_{0.02})_{0.92}Sn_{0.08}]O_3 = (Pb_{0.97}Ba_{0.03})(Zr_{0.902}Ti_{0.018}Sn_{0.08})O_3$

* UNIVERSITY OF SILESIA, FACULTY OF COMPUTER SCIENCE AND MATERIALS SCIENCE, MATERIALS SCIENCE DEPARTMENT, 2 ŚNIEŻNA STR., 41-200 SOSNOWIEC, POLAND
** INSTITUTE OF MATERIALS SCIENCE, 75 PUŁKU PIECHOTY 1A STR., 41-500 CHORZÓW, POLAND

2. Samples and experiment

In order to avoid a deficit of lead during the high temperature sintering the excess of PbO has been added in the amount of about 5%. Then, the powders were subjected to complete mixing and wet-milling process in a planetary ball mill for 15 hours at a speed of 200 rpm. In the next stage, the dried powders were calcined at a temperature of T_{calc} = 850°C for 3 hours. After calcination the powders were mixed for 2 hours. The obtained powders were formed into pellets using a hydraulic press by cold pressing method under a pressure of 250 MPa. Next, the pallets were sintered in the conditions of T_s = 1250°C for 4 hours using free sintering method.

3. Results and discussion

The first stage of the study was the analysis of the chemical composition by EDS technique using NORAN VANTAGE equipment. The example of EDS spectrum for PBZTS ceramics with z =0.08 is shown in Fig. 1.

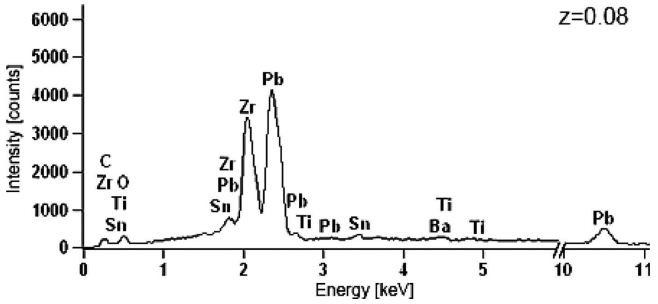

Fig. 1. The example of EDS spectrum for $(Pb_{0.97}Ba_{0.03})[(Zr_{0.98}Ti_{0.02})_{0.92}Sn_{0.08}]O_3$ sample

The obtained EDS spectra (Fig. 1) excluded the presence of foreign elements or impurities. The amount of the individual elements calculated from these EDS spectra (points) was compared with the assumed values (lines). The results are shown in Fig. 2. It is seen from this figure a slight deficit of lead and slight excess of zirconium. It means that the introduction of 5% excess of lead oxide during weighing probably do not compensate the loss of lead during sintering at high temperature.

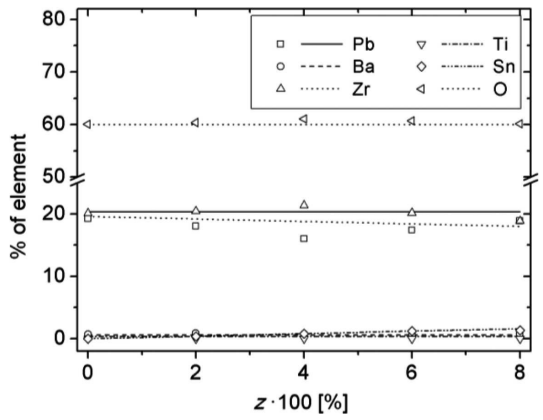

Fig. 2. Chemical composition of investigated $(Pb_{0.97}Ba_{0.03})[(Zr_{0.98}Ti_{0.02})_{1-z}Sn_z]O_3$ samples (lines – assumption, points – experimental EDS results)

The microstructure of fractured samples was investigated using HITACHI S-4700SEM scanning electron microscope. The results are presented in Fig. 3.

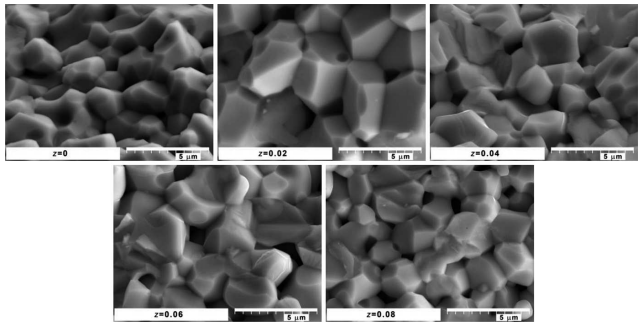

Fig. 3. SEM images of fractured $(Pb_{0.97}Ba_{0.03})[(Zr_{0.98}Ti_{0.02})_{1-z}Sn_z]O_3$ samples

From the analysis of images presented in Fig. 3 we can state that the investigated ceramics are characterized by a fairly large porosity and quite fine grains as compared to ceramics studied in works [9, 10]. On all photographs in some places we can observe cracking through the grains. This effects is the most apparent for ceramics with 6% stannate. We also observed the following influence of stannate on the grain size: for z =0 grains have a small size, for z =0.02 grains have the largest size and then grain size gradually decreases with increasing z.

The XRD measurements were performed using a Philips diffractometer and CuK_α filtered radiation and the step 0.05 deg. The X-ray diffraction patterns of the powders after calcination are shown in Fig. 4a, and the finally sintered ceramics in Fig. 4b. It can be seen that the obtained PBZTS samples

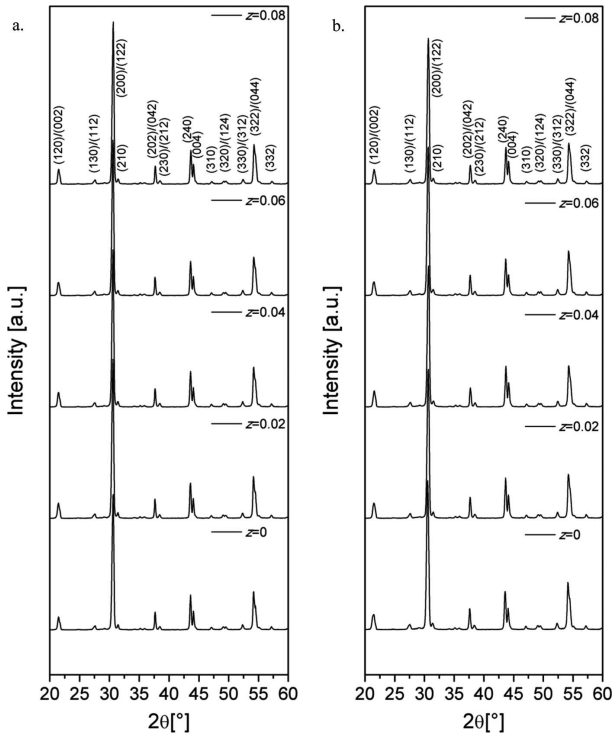

Fig. 4. XRD diffraction patterns of $(Pb_{0.97}Ba_{0.03})[(Zr_{0.98}Ti_{0.02})_{1-z}Sn_z]O_3$ ceramics at room temperature: a – powders after calcination (orthorhombic phase); b – finally sintered ceramics (orthorhombic phase)

after the sintering are free of unwanted pyrochlore phase, and all the diffraction lines correspond to the perovskites phase. The indexing the diffraction lines (Fig. 4) was conducted on the basis of a standard for $PbZrO_3$ phase (ICDD PDF 01-087-0568).

All sintered samples are predominantly orthorhombic but some additional phase can probably be also present what is seen from Fig. 5. The analysis of the enlarged fragments of diffraction patterns for the sintered PBZTS ceramics (z =0 and z =0.08) corresponding to the lines (240/004) the orthorhombic phase (for the rhombohedral phase at this point is a line (200)) shows that it is possible to identify three diffraction lines, but the third component has a low intensity. This suggests the presence in both cases the phase other than the orthorhombic one (for example PbO phase). Fig. 4 shows also the superlattice reflections (for example 230/212), which may suggest that the sintering process did not lead to the finishing of reactions in final ceramic.

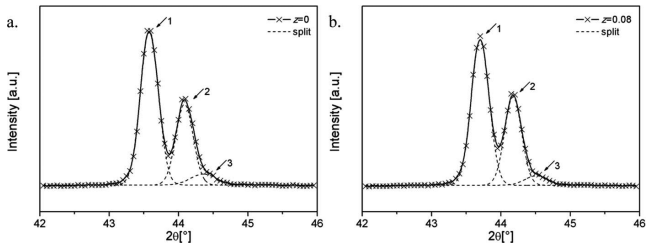

Fig. 5. Comparison of fragments of X-ray diffraction patterns corresponding to the lines (240/004) of the orthorhombic phase for sintered ceramics: a – z =0, b – z =0.08.
Dashed lines – the result of splitting on the three individual peaks, solid line – experimental curve

On the base of the diffraction patterns the unit cell parameters were calculated by Rietveld method and are presented in Table 2. The Fig. 6 shows the dependence the lattice parameters (a, b, c) on the z and Fig. 7 shows the dependence of unit cell volume on the z.

TABLE 2
The unit cell parameters and the volume of unit cell for PBZTS ceramics

PBZTS	Space group	a [nm]	b [nm]	c [nm]	V [nm^3]
z =**0**	*Pbam (55)*	0.58747(2)	1.17680(4)	0.82221(3)	0.56842
z =**0.02**	*Pbam (55)*	0.58724(2)	1.17660(4)	0.82225(3)	0.56813
z =**0.04**	*Pbam (55)*	0.58700(2)	1.17612(4)	0.82208(3)	0.56755
z =**0.06**	*Pbam (55)*	0.58670(2)	1.17542(4)	0.82174(3)	0.56669
z =**0.08**	*Pbam (55)*	0.58640(2)	1.17490(4)	0.82154(3)	0.56601

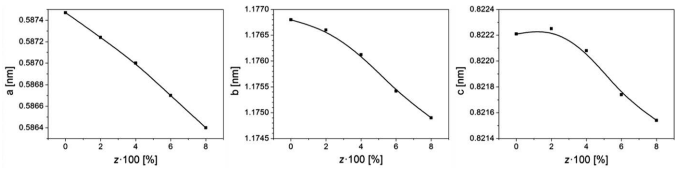

Fig. 6. The dependence the lattice parameters (a, b, c) on the z. The uncertainties of cell parameters are shown in Table 2

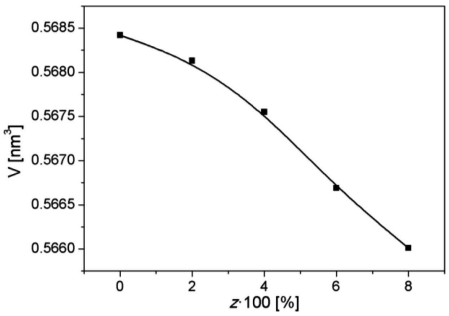

Fig. 7. The dependence of unit cell volume on the z. The uncertainty of the unit cell volume is about ±0.015%

Our conclusion is following - the increase of content of stannate reduce the size of the unit cell. This may be connected with the fact that the ionic radius of Sn^{4+} (r_i = 0.074 nm) is smaller than the Zr^{4+} (r_i = 0.087 nm). Radius of titanium ion (r_i = 0.061 nm) is smaller than the tin ion, but in the investigated samples titanium is in a small amount. The results shown in Fig.6 and Fig.7 are similar to the result obtained in the work [11] for the PBZT ceramics.

Dielectric permittivity v.s. temperature (during heating) has been measured using BR-2817 LCR-meter at the temperature range from 20°C to 327°C. Obtained as a result dependencies of dielectric permittivity on temperature are presented in Fig. 8a and $tan\delta(T)$ in Fig. 8b.

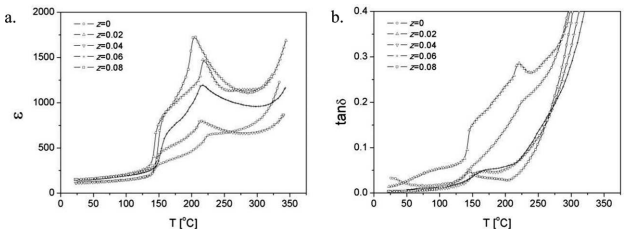

Fig. 8. The temperature dependencies of $\varepsilon'(T)$ and $tan\delta(T)$ for frequency 1kHz: a) dielectric permittivity; b) dielectric loss tangent

All temperature dependencies of dielectric permittivity (Fig. 8a) exhibit two anomalies, but there was no clear relation between value of z and the degree of diffusion of the dielectric permittivity. The dependence of $T_m(z)$ was determined from the data in Fig. 8a and shown in Fig. 9. The temperature in which there is the maximum of dielectric permittivity decreases with increasing content of stannate, however, there was no clear relation between the value of z and the shape and position of the maximum of the dielectric loss tangent (Fig. 8b).

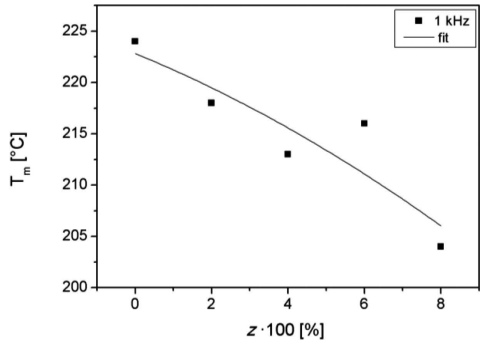

Fig. 9. The dependency $T_m(z)$ for $(Pb_{0.97}Ba_{0.03})[(Zr_{0.98}Ti_{0.02})_{1-z}Sn_z]O_3$ ceramics

$P-E$ hysteresis loops have been investigated using virtual Sawyer-Tower's bridge with HEOPS-5B6 high voltage amplifier. Results are presented in Fig. 10 for frequency ν =10 Hz. For all investigated samples ferroelectric hysteresis loops are not observed at low temperatures. The dependence of $P(E)$ at low temperatures is rather typical for linear dielectrics. The ferroelectric hysteresis loops appear only at high temperatures (above 80°C). Loops become progressively narrower during further increase of temperature (ie, coercive field decreases) and at the same time polarization increases (loops are higher). The hysteresis loop for sample with z =0 is the widest of all, i.e. with the increase of z the ferroelectric hardness of material decreases.

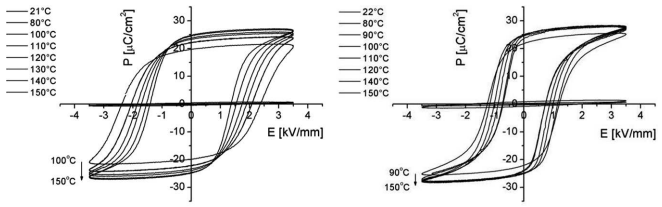

Fig. 10. P–E hysteresis loops for investigated $(Pb_{0.97}Ba_{0.03})[(Zr_{0.98}Ti_{0.02})_{1-z}Sn_z]O_3$ ceramics (frequency of measurements – 10Hz): a – z =0; b – z =0.08

The analysis of the dependency $E_C(T)$ (Fig. 11a) suggest that the initial increase of the coercive field with increasing temperature can be seeming and is probably related to electrical conductivity. The remnant polarization (P_r) was estimated from the data $P(E)$ and is shown in Fig. 10b. Also in this case, only at higher temperatures (above approximately 80°C) we can observe qualitative change of the dependence $P_r(T)$. G. Shirane obtained a similar effect in work [12] in $(Pb_{1-x}Ba_x)ZrO_3$ solid solution. This effect was explained as the antiferroelectric-ferroelectric-paraelectric phase transitions (going towards high temperatures).

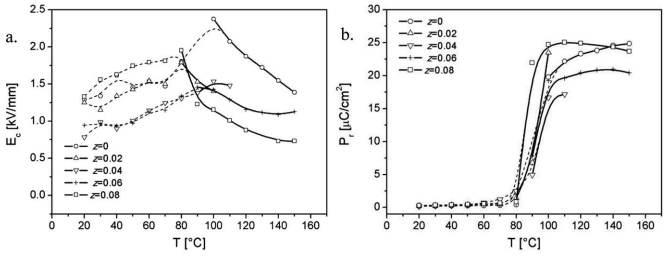

Fig. 11. The temperature dependencies for frequency 10Hz: a – $E_C(T)$; b – $P_r(T)$

4. Conclusions

SEM studies show that the obtained ceramic samples have a relatively large porosity and quite fine grains. The best shaped grains are in ceramics with z =0.02. There was no clear relation between the content of stannate and the shape of the grains. The EDS spectra analysis shows that in all obtained and investigated samples occur a slight deficit of lead and excess of zirconium. With the increasing content of stannate all unit cell parameters decrease.

All graphs $\varepsilon'(T)$ and $1/\varepsilon'(T)$ exhibit two anomalies. There was no clear relation between content of stannate and the degree of diffusion of the maximum of dielectric permittivity. Also the influence of frequency of the measuring field on the temperature (T_m) is not clear. It can be stated from obtained dielectric measurements that the phase transition from the ferroelectric phase to the paraelectric one occurs at temperatures from about 200°C to about 225°C.

The hysteresis loops appear only at high temperatures (above approximately 80°C). It may be caused by the occurrence of the antiferroelectric-ferroelectric-paraelectric phase transitions (during heating).

So, it can be concluded that the addition of stannate to the PBZT causes some changes of the parameters which may be relevant for applications, for example shift the temperature T_m, the increase of diffusion of the maximum of dielectric permittivity, etc. It also allows to control the shape of the hysteresis loops.

REFERENCES

[1] R. Skulski, Diffused phase transitions in selected groups of ferroelectrics and relaxors, University of Silesia, Katowice 1999 (in Polish).
[2] R. Skulski, E.G. Fesenko, Z. Surowiak, Ferroelectric Letters **28**, 145-153 (2001).
[3] R. Zachariasz, D. Bochenek, Arch. Metall. Mater. **54**, 895-902 (2009).
[4] D. Bochenek, R. Zachariasz, Arch. Metall. Mater. **54**, 903-910 (2009).
[5] T. Ikeda, J. Phys. Soc. Japan **14**, 168-174 (1959).
[6] G. Li, G.H. Haertling, Ferroelectrics **166**, 31-45 (1995).
[7] Z. Ujma, M. Adamczyk, J. Handerek, J. Eur. Ceram. Soc. **18**, 2201-2007 (1998).
[8] J. Handerek, M. Adamczyk, Z. Ujma, Ferroelectrics **233**, 253-270 (1999).
[9] D. Brzezińska, R. Skulski, P. Wawrzała, Arch. Metall. Mater. **56**, 1243-1247 (2011).
[10] D. Bochenek, R. Skulski, P. Wawrzała, D. Brzezińska, Ferroelectrics **418**, 82-87 (2011).
[11] T. Bongkarn, Ch. Thiangchit, Ferroelectrics **383**, 78-83 (2009).
[12] G. Shirane, Phys. Rev. **86**, 219-227 (1952).

Received: 20 September 2013.